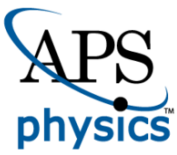

Giant Amplification of Noise in Fluctuation-Induced Pattern Formation

Tommaso Biancalani, Farshid Jafarpour, and Nigel Goldenfeld

Phys. Rev. Lett. **118**, 018101 — Published 3 January 2017

DOI: 10.1103/PhysRevLett.118.018101

Giant amplification of noise in fluctuation-induced pattern formation

Tommaso Biancalani,* Farshid Jafarpour,† and Nigel Goldenfeld
Department of Physics, University of Illinois at Urbana-Champaign, Loomis Laboratory of Physics, 1110 West Green Street, Urbana, Illinois, 61801-3080. and Carl R. Woese Institute for Genomic Biology, University of Illinois at Urbana-Champaign, 1206 West Gregory Drive, Urbana, Illinois 61801.
(Dated: December 12, 2016)

The amplitude of fluctuation-induced patterns might be expected to be proportional to the strength of the driving noise, suggesting that such patterns would be difficult to observe in nature. Here, we show that a large class of spatially-extended dynamical systems driven by intrinsic noise can exhibit giant amplification, yielding patterns whose amplitude is comparable to that of deterministic Turing instabilities. The giant amplification results from the interplay between noise and nonorthogonal eigenvectors of the linear stability matrix, yielding transients that grow with time, and which, when driven by the ever-present intrinsic noise, lead to persistent large amplitude patterns. This mechanism shows that fluctuation-induced Turing patterns are observable, and are neither strongly limited by the amplitude of demographic stochasticity nor by the value of the diffusion coefficients.

PACS numbers: 05.40.Ca, 87.10.Mn, 87.23.Cc, 02.50.Ey, 87.18.Hf

Since the seminal paper of Turing [1], it has been recognized that pattern forming dynamical instabilities could potentially underlie various examples of biological pattern formation and development [2, 3]. The Turing mechanism has two major assumptions: first, that two chemical species behave as an activator-inhibitor system (but see a recent extension [4]), and secondly, that the spatial diffusion constant of the inhibitor is greater than that of the activator, typically by two orders of magnitude or more [5, 6]. However, this second condition is not generally present in experimental observations [7, 8]. The widely-held conclusion is that biological patterns reflect gene expression and the interplay of developmental processes, so that the Turing mechanism itself is not generally operative [9].

This conclusion relies upon a third assumption of Turing patterns: that they are deterministic. However, many biological systems exhibit strong fluctuations due to demographic stochasticity (or small number fluctuations), arising from (e.g.) finite population size (ecology) or copy number (gene expression) [10, 11], and these fluctuations could potentially couple to the underlying pattern-forming instabilities. Detailed analysis shows that the length scale of fluctuation-induced patterns is set by the same condition as in the deterministic Turing analysis, but remarkably the pattern exists over a wide range of parameter values, even where the diffusion constants of activator and inhibitor are of similar magnitudes [5, 12–17]. These fluctuation-induced or stochastic patterns arise physically because, even though the uniform unpatterned state is linearly stable, the demographic fluctuations are constantly pushing the system slightly away from its stable fixed point; if the resulting small amplitude dynamics is dominated by an eigenvalue with a nonzero wavelength, then a spatial pattern can arise.

Unfortunately, this mechanism suggests that the amplitude of fluctuation-induced patterns would be set by $\Omega^{-1/2}$, where Ω indicates the total number of molecules within a correlation volume of the system, i.e. the spatial patch within which the system can be considered to be well mixed [12, 13]. Thus in situations where $\Omega \gg 1$, fluctuation-induced patterns would have a very small amplitude compared to deterministic Turing patterns, and so might not be observable nor relevant to biological and ecological pattern formation [18].

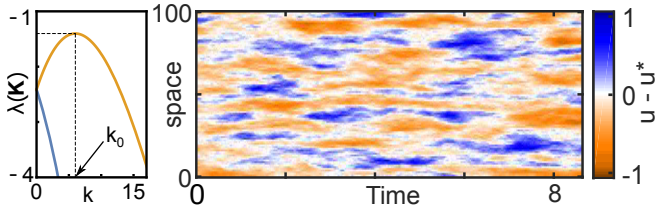

FIG. 1. **(Color online) Turing-like pattern with large amplitude and comparable diffusivities**. (right panel) Stochastic simulations [19] of a two-species model (8) with diffusivities $\delta_U = 3.9$, $\delta_V = 3.4\,\delta_U$ and system size $\Omega = 10^4$. Patterns are noise-induced as they arise from a stable homogeneous state u^*, *i.e.*, the eigenvalues λ plotted against the wavelength k are negative (left panel). However, the pattern amplitude results of the order of one (right bar). Other parameters: $a = 3$, $b = 5.8$, $c = e = 1$.

The purpose of this Letter is to show that fluctuation-induced Turing patterns can in fact be readily observed, even when the noise is very small and the ratio of diffusion constants is close to one. The new ingredient to the theory uncovered here is the presence of giant amplification, due to an interplay between demographic stochasticity and nonorthogonality of the eigenvectors of the linear stability operator about the uniform stable steady state. In the related problem of noise-induced population cycles in predator-prey systems, amplification arises

due to a resonance of the noise with a complex eigenvalue arising from the linearized stability about the time-independent state [20]. In fluctuation-induced stationary Turing patterns, this mechanism cannot be relevant, because the eigenvalues are real, not complex, and so there can be no resonant amplification [12, 13]. Our analytical theory shows that giant amplification occurs in a wide class of fluctuation-induced pattern-forming systems, and is a source of amplification distinct from the population size dependent resonance that was already identified to arise in spatially-uniform quasicycles [20].

An example of our key result described below is shown in Fig. 1: stochastic simulations of the generic pattern-forming model of Ridolfi et al. [21], performed on a linear chain of 10^2 spatial cells, each cell with a system size of $\Omega = 10^4$. Patterns are noise-induced as they arise from a stable homogeneous state (left panel), but despite the factor $\Omega^{-1/2} = 10^{-2}$ the resulting amplitude is of order unity.

This giant amplification is due to the counterintuitive fact that the dynamics following a small displacement from a stable fixed point need not relax back to the fixed point monotonically: there can be an initial transient amplification if the linear stability matrix is nonnormal: that is, it does not admit an orthogonal set of eigenvectors (Fig. 2). Nonnormality has been thoroughly investigated at a deterministic level in fluid dynamics [22–24], and in ecology [25, 26], and is a common feature of pattern-forming systems [21, 27, 28]. The specific contribution of the present paper is to systematically analyze the behavior of nonnormal systems in the presence of intrinsic noise. Numerical results of shear flow turbulence [29] indicate that nonnormality can increase the variance of stochastic forcing in well-mixed systems, yet an analytical treatment is still missing. Our work treats the role of nonnormality in fluctuation-induced spatial patterns, and shows that its widespread occurrence suggests a new way in which fluctuation-induced Turing patterns are amplified and thus potentially play a wider role in biological and ecological pattern formation than previously recognized.

Nonnormality in stochastic dynamics:- We begin by quantifying the degree of amplification in a well-mixed stochastic system. Consider the linear stochastic differential equation for an m-component state vector $\vec{y}$:

$$\dot{\vec{y}} = \boldsymbol{A}\,\vec{y} + \sigma\,\vec{\eta}(t), \tag{1}$$

where the components of $\vec{\eta}$, are normalized Gaussian white noises and the model-dependent matrix $\boldsymbol{A}$ has negative real eigenvalues, λ_i $(i = 1, \ldots, m)$. Therefore, the fixed point $\vec{y}_0 = 0$ is stable. The coefficient σ represents the strength of the fluctuations and scales with the system size $\Omega^{-1/2}$ in the case of demographic noise. Equation (1) is the prototypical linearization of stochastic dynamics near a stable fixed point, and we analyze the mean squared displacement from the fixed point, $\left\langle \|\vec{y}\|^2 \right\rangle$, where $\|\vec{y}\| = \sqrt{\vec{y}^T\vec{y}}$, is the Euclidean norm.

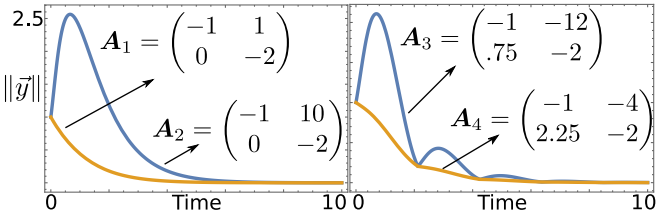

FIG. 2. **(Color online) Stable linear systems can amplify perturbations [25].** Dynamics of the Euclidean norm $\|\vec{y}\|$ obtained by solving $\dot{\vec{y}} = \boldsymbol{A}_i\vec{y}$. Reactive systems exhibit transient amplification before relaxing to fixed point (blue lines), in contrast with conventional response of stable systems (yellow lines). Matrices $\boldsymbol{A}_1$ and $\boldsymbol{A}_2$ (respectively $\boldsymbol{A}_3$ and $\boldsymbol{A}_4$) have same real (respectively complex conjugate) eigenvalues.

Since all the eigenvalues of $\boldsymbol{A}$ are negative, under the deterministic part of Eq. (1), all the components of $\vec{y}$ decay exponentially to zero along the eigenvectors of $\boldsymbol{A}$, with decay time scales $\tau_i = \lambda_i^{-1}$. In contrast, the noise term provides stochastic agitation with a strength proportional to σ. One might intuitively expect that an upper bound for $\left\langle \|\vec{y}\|^2 \right\rangle$ could be found by replacing all the eigenvalues by the eigenvalues corresponding to the slowest decaying mode, $\lambda = \max\{\lambda_i\}$. Therefore, the norm of $\vec{y}_u$ with the dynamics $\dot{\vec{y}}_u = \lambda\,\vec{y}_u + \sigma\,\vec{\eta}(t)$, should provide an upper bound for $\|\vec{y}\|$. The mean squared norm of $\vec{y}_u$ is readily given by $\left\langle \|\vec{y}_u\|^2 \right\rangle = m\lambda^{-1}\sigma^2/2$.

However, this upper bound is only valid when the matrix $\boldsymbol{A}$ is normal, *i.e.* it has an orthogonal set of eigenvectors [29]. This can be understood by analyzing the behavior of Eq. (1) in the deterministic limit ($\sigma = 0$). Although the asymptotic decay rate of $\|\vec{y}\|$ is set by the eigenvalues of $\boldsymbol{A}$, the instantaneous response is given by the eigenvalues of $\boldsymbol{H} = (\boldsymbol{A} + \boldsymbol{A}^T)/2$, the Hermitian part of $\boldsymbol{A}$ [25]. If $\boldsymbol{A}$ is nonnormal, then the short-time dynamics of $\|\vec{y}\|$ cannot be predicted by the eigenvalues of $\boldsymbol{A}$. Remarkably, $\boldsymbol{H}$ can admit positive eigenvalues even though $\boldsymbol{A}$ possesses all negative eigenvalues, in which case $\|\vec{y}\|$ can experience a transient growth, for suitable initial conditions, before it starts decaying (Fig. 2). This mechanism, sometimes termed as reactivity [25], occurs because the transformation that takes $\vec{y}$ to the eigenbasis of $\boldsymbol{A}$ is not unitary if the eigenvectors of $\boldsymbol{A}$ are not orthogonal, and thus does not preserve the norm of $\vec{y}$. Clearly, if the stable matrix amplifies perturbations, the previous bound cannot hold.

In the presence of noise, the transient amplification in the deterministic part of Eq. (1) has a lasting effect on the steady state amplitude of the stochastic dynamics. We demonstrate this by computing the mean squared norm for Eq. (1) (see the detailed derivation in the Supplemen-

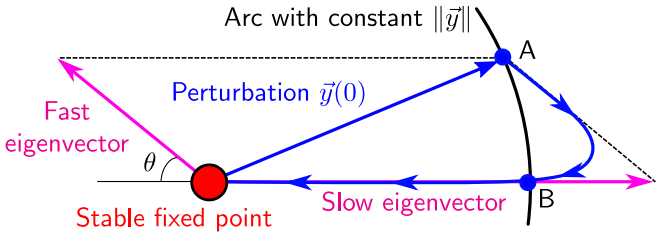

FIG. 3. **(Color online) Transient amplification is caused by nonorthogonal eigenvectors and a separation of timescales**. The stable fixed point is subject to the perturbation $\vec{y}(0)$. Because of the separation of timescales, the deterministic trajectory (blue arrowed line) is initially parallel to the fast eigenvector before relaxing to the slow manifold. From A to B, the trajectory has magnitude greater than $||\vec{y}_0||$.

tal Material (SM) [30]):

$$\left\langle \|\vec{y}\|^2 \right\rangle = -\frac{\sigma^2}{2}\mathcal{H}(\boldsymbol{A})\,\mathrm{tr}\left(\boldsymbol{A}^{-1}\right), \tag{2}$$

where tr stands for the trace function and we define $\mathcal{H}$ as the nonnormality index. The term $\mathrm{tr}\left(\boldsymbol{A}^{-1}\right)$ is the conventional term that accounts for the matrix stability: the more stable the matrix, the smaller the mean squared norm of $\vec{y}$ due to stochastic forcing. In contrast, the nonnormality index is a real number always $\mathcal{H} \geq 1$, and is equal to one if and only if the matrix $\boldsymbol{A}$ admits a basis of orthogonal eigenvectors. This is the term that accounts for amplification due to the nonnormality of matrix $\boldsymbol{A}$, and indeed, the further $\boldsymbol{A}$ is from normal, the larger is the index $\mathcal{H}$. We can obtain intuition about the nonnormality index in the case of a two-dimensional matrix $\boldsymbol{A}$, where the nonnormality index $\mathcal{H}$ simplifies to the following simple expression, where $\cot\theta$ is the cotangent of the angle between the two eigenvectors (see SM for derivation and general formulae):

$$\mathcal{H} = 1 + \cot^2(\theta)\left(\frac{\lambda_1 - \lambda_2}{\lambda_1 + \lambda_2}\right)^2. \tag{3}$$

This expression gives us quantitative understanding about how transient amplification occurs (Fig. 3). Two ingredients are necessary: nonorthogonal eigenvectors and a separation of time scales given by eigenvalues of different magnitudes. If the system is not subject to noise, suitable initial conditions are also required (*e.g.* the blue vector in Fig. 3). Because of the separation of time scales, the component of $\vec{y}$ along the eigenvector associated with the faster eigenvalue decays quickly, whereas in the slow direction the dynamics is approximately constant. However, because of nonorthogonality, the norm of $\vec{y}$ instantaneously increases as $\vec{y}$ moves along the fast eigenvector, until the slow manifold starts attracting the trajectory back to fixed point.

Nonnormality in spatially-extended pattern formation:- We now analyze spatially-extended, diffusively-coupled pattern-forming systems driven by noise. Specifically, we consider the generic equation

$$\frac{\partial \vec{q}}{\partial t} = \vec{f}(\vec{q}) + \boldsymbol{D}\nabla^2\vec{q} + \sigma\vec{\xi}(\vec{x},t), \tag{4}$$

where $\vec{x}$ is a space variable, the vector $\vec{q} = (q_1, q_2)$, the diffusion matrix $\boldsymbol{D} = \mathrm{diag}(D_1, D_2)$, and ξ_i's, the components of $\vec{\xi}(\vec{x},t)$ are normalized δ-correlated Gaussian white noises. Also, we assume that $\vec{f}(\vec{q})$ has a stable fixed point $\vec{q}^*$, and all of the eigenvalues of the linear stability or Jacobian matrix $\boldsymbol{J} = \nabla_{\vec{q}} f(\vec{q})|_{\vec{q}^*}$ have negative real part.

We first show that in the presence of noise, system (4) exhibits patterns in a parameter regime where the fixed point $\vec{q}^*$ is stable. The stability of $\vec{q}^*$ can be inspected by defining the deviation $\vec{p} = \vec{q} - \vec{q}^*$ and linearizing near $\vec{q}^*$, yielding

$$\frac{\partial \vec{p}}{\partial t} = \boldsymbol{J}\vec{p} + \boldsymbol{D}\nabla^2\vec{p} + \sigma\vec{\xi}(\vec{x},t). \tag{5}$$

The spatial degrees of freedom can be diagonalized by a Fourier transform ($\vec{x} \mapsto \vec{k}$), resulting in

$$\frac{\mathrm{d}\vec{p}_{\vec{k}}}{\mathrm{d}t} = \boldsymbol{K}\vec{p}_{\vec{k}} + \sigma\vec{\xi}(\vec{k},t), \qquad \boldsymbol{K} = \boldsymbol{J} - k^2\boldsymbol{D}. \tag{6}$$

Equation (6) is a complex version of Eq. (1).

We start by reviewing the stability of the deterministic part of Eq. (5). If $D_1 = D_2$, matrix $\boldsymbol{D}$ is a multiple of the identity, and the eigenvalues of $\boldsymbol{K}$ will be the eigenvalues of $\boldsymbol{J}$ shifted by $-k^2D$ for each $\vec{k}$, resulting in a more stable operator. However, in the case that the diffusion rates are sufficiently different, the largest eigenvalue of $\boldsymbol{K}$ can have a nonmonotonic behavior as a function of k^2, and in some cases have positive eigenvalues for a small range of $\vec{k}$ peaked around some nonzero value $\vec{k}_0$. In this case, the modes near $\vec{k}_0$ will grow leading to the formation of deterministic Turing patterns [1]. Therefore, the formation of deterministic Turing patterns is dependent on a large separation of the diffusion constants [6–8].

In contrast, consider an intermediate scenario with diffusion constants different enough so that they can cause a nonmonotonic behavior for the largest eigenvalue of $\boldsymbol{K}$ as a function of k^2 peaked around some value $\vec{k}_0$, but not enough for the largest eigenvalue to be positive at $\vec{k}_0$ (left panel of Fig. 1). In this case, all the $\vec{k}$ modes decay quickly to zero, but the modes with $\vec{k} \sim \vec{k}_0$ decay slower than the others, causing a transient pattern. In the presence of the noise term $\vec{\xi}(\vec{k},t)$ in Eq. (6), while the modes with smaller eigenvalues decay quickly to zero, the slow modes drift away from the fixed point under the influence of the noise. The drift of the $\vec{k}$ modes near $\vec{k}_0$ produces persistent steady-state fluctuation-induced patterns with well-defined length-scales [12, 13]. While the stochastic Turing patterns have a less stringent requirement than

the deterministic Turing patterns for the ratio of the diffusion constants, their amplitude is limited to the amplitude of the drift under the noise suppressed by the slow deterministic decay. As discussed in the previous section, the mean squared amplitude is of order $\lambda^{-1}\sigma^2$, unless we can show that the system is nonnormal.

We now show that in order for a system described by Eq. (4) to produce stochastic patterns, it is necessary for the matrix $\boldsymbol{J}$ in Eq. (5) to be nonnormal. The real part of the largest eigenvalue of a normal matrix is equal to that of its hermitian part. Therefore, we can measure how far from normal the matrix $\boldsymbol{J}$ is by finding a lower bound on the difference between the largest eigenvalue of $\boldsymbol{H} = (\boldsymbol{J} + \boldsymbol{J}^T)/2$ and that of matrix $\boldsymbol{J}$ (the proof of this inequality is given in SM):

$$\lambda_1(\boldsymbol{H}) - \Re(\lambda_1(\boldsymbol{J})) \geq \delta + k_0^2 D_{min}, \tag{7}$$

where $\delta = \Re(\lambda_1(\boldsymbol{K}(\vec{k}_0))) - \Re(\lambda_1(\boldsymbol{J})) > 0$, $\vec{k}_0$ is the wave vectors at which the real part of the largest eigenvalue peaks, and D_{min} is smallest of the diffusion constants.

Since the nonnormality of $\boldsymbol{J}$ should be independent of the diffusion constants, this lower bound can be extended to the supremum of the right hand side of the inequality (7) over all the matrices $\boldsymbol{D}$ that produce spatial patterns and their corresponding $\vec{k}_0$. In particular, if a system admits deterministic Turing patterns for some set of diffusion constants, this inequality implies that the matrix $\boldsymbol{J}$ would be reactive (*i.e.* $\lambda_1(\boldsymbol{H}) \geq 0$. this special case was previously proven by Neubert et al. [27]). In this case, if experimentally measured values of diffusion constants do not fall within the Turing pattern regime, the system is still reactive and capable of exhibiting amplified stochastic patterns.

A worked-out example :- Finally, we apply our theory to a concrete model that is representative of a large class of systems. The model is given by Eq. (4) with two species U and V with densities $\vec{q} = (u, v)$, and $\vec{f}(u, v) = \big(u(auv - e),\ v(b - cu^2 v)\big)$, with $a, b, c, e > 0$ [21]. The corresponding individual-level model is defined by considering the following reactions that occur on a discretized m-dimensional space with L^m lattice sites,

$$\begin{aligned} &2U_i + V_i \xrightarrow{a} 3U_i + V_i, \qquad V_i \xrightarrow{b} 2V_i, \\ &U_i \xrightarrow{e} \varnothing, \qquad 2V_i + 2U_i \xrightarrow{c} V_i + 2U_i, \\ &U_i \xrightarrow{\delta_U} U_j, \qquad V_i \xrightarrow{\delta_V} V_j, \qquad j \in \langle i \rangle \end{aligned} \tag{8}$$

where U_i and V_i are the species U and V on the site i for $i = 1 \ldots L^m$ and $\langle i \rangle$ is the set of sites neighboring i. The state of the system is specified by the concentration vectors $\vec{q}_i \equiv (u_i, v_i) \equiv (U_i, V_i)/\Omega$, where Ω is the volume of each site. The diffusion rates δ_u and δ_v are related to the diffusion constants by $(\delta_u, \delta_v) = (D_U, D_V)/\Omega^{2/m}$. The discrete-space version of Eqs. (4), (5) and (6) are derived by expanding in powers of $\Omega^{-1/2}$ the master equation

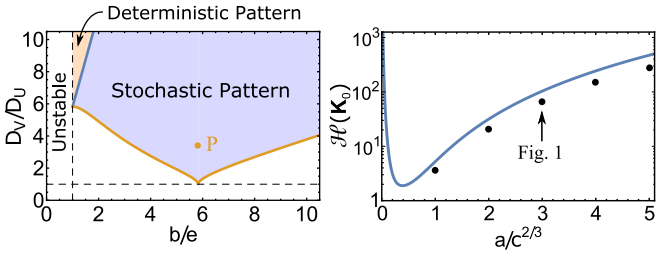

FIG. 4. **(Color online) Stochasticity allows pattern formation for similar diffusivities**. (left) Phase diagram of model (8) showing that the pattern forming behavior of this model depends only on the ratios b/e and D_V/D_U (see SM for analytical expression for the boundaries). (right) Semi-log plot of nonnormality index for the point P as a function of $a/c^{2/3}$. Black markers are amplifications measured in simulations.

corresponding to scheme (8) (see the SM for the derivations).

The pattern forming behavior of the model described by (8) only depends on the ratio of the diffusion constants D_V/D_U and the ratio of the reaction rates of the two linear reactions b/e. The left panel of Fig. 4 shows the regime of parameters in which the system exhibits either stochastic or deterministic Turing patterns [31]. As expected, deterministic patterns emerge only when the ratio D_V/D_U of diffusion constants is very large (above the blue line in Fig. 4 which grows rapidly outside of the figure), while the requirement on this ratio for the stochastic patterns is drastically reduced. In the absence of the nonnormality effect, one would expect that only stochastic patterns with parameters very close to the deterministic regime would be observed, since far from this regime, the amplitude of the patterns would be too small to detect.

However, since for all $b/e > 1$, there is a D_V/D_U above which the system exhibits deterministic Turing patterns, $\boldsymbol{J}$ is reactive. Therefore, even when the system is far from the parameter regime of deterministic patterns, the amplitude of the stochastic patterns is far larger than what one would expect from the analysis of the eigenvalues. We can see this by analyzing the amplitude of the patterns at the point P in Fig. 4. This point ($b/e = 5.8$ and $D_V/D_U = 3.4$) is chosen to be very far from the deterministic Turing pattern regime. At this b/e ratio, the ratio of the diffusion constants has to be at least ten times larger for the system to exhibit deterministic Turing patterns. The amplitude of the patterns as determined by Eq. (2) is dependent on the eigenvalues of $\boldsymbol{K}$ (fixed by the choice of the point P) and the nonnormality index $\mathcal{H}(\boldsymbol{K})$ which can be tuned by changing the ratio $a/c^{2/3}$ without changing the point P. The right panel of Fig. 4 shows that the amplification of stochastic patterns for the point P varies over orders of magnitude for a small range of $a/c^{2/3}$.

The right panel of Fig. 1 shows the time series of the amplified stochastic Turing patterns in the concentration of the species U, in a simulation of our model in one dimension (for the point specified in the right panel of Fig. 4). The mean squared amplitude of these spatial patterns is about 0.21, while the upper bound for the amplitude of the pattern in the absence of nonnormality is 2.5×10^{-3}. The nonnormality index $\mathcal{H}$ (of the slowest Fourier mode $k_0 = 6$) is about 103 justifying the two order of magnitude amplification in the amplitude of the stochastic patterns.

This work was supported by the National Aeronautics and Space Administration Astrobiology Institute (NAI) under Cooperative Agreement No. NNA13AA91A issued through the Science Mission Directorate. T.B acknowledges partial funding from the National Science Foundation under Grant No. PHY-105515.

* Present address: Physics of Living Systems, Department of Physics, Massachusetts Institute of Technology, Cambridge, MA

† T. Biancalani and F. Jafarpour contributed equally to this work.

[1] A. M. Turing, Philos. Trans. R. Soc. London, Ser. B **237**, 37 (1952).
[2] A. Koch and H. Meinhardt, Rev. Mod. Phys. **66**, 1481 (1994).
[3] A. D. Economou, A. Ohazama, T. Porntaveetus, P. T. Sharpe, S. Kondo, M. A. Basson, A. Gritli-Linde, M. T. Cobourne, and J. B. Green, Nature genetics **44**, 348 (2012).
[4] S. Werner, T. Stückemann, M. B. Amigo, J. C. Rink, F. Jülicher, and B. M. Friedrich, Phys. Rev. Lett. **114**, 138101 (2015).
[5] T. Butler and N. Goldenfeld, Physical Review E **84**, 011112 (2011).
[6] J. D. Murray, *Mathematical Biology. II Spatial Models and Biomedical Applications* {*Interdisciplinary Applied Mathematics V. 18*} (Springer-Verlag New York Incorporated, 2001).
[7] V. Castets, E. Dulos, J. Boissonade, and P. De Kepper, Phys. Rev. Lett. **64**, 2953 (1990).
[8] Q. Ouyang and H. L. Swinney, Nature **352**, 610 (1991).
[9] P. K. Maini, T. E. Woolley, R. E. Baker, E. A. Gaffney, and S. S. Lee, Interface focus , rsfs20110113 (2012).
[10] M. Mobilia, I. T. Georgiev, and U. C. Täuber, Journal of Statistical Physics **128**, 447 (2007).
[11] F. Jafarpour, T. Biancalani, and N. Goldenfeld, Phys. Rev. Lett. **115**, 158101 (2015).
[12] T. Butler and N. Goldenfeld, Phys. Rev. E **80**, 030902 (2009).
[13] T. Biancalani, D. Fanelli, and F. Di Patti, Phys. Rev. E **81**, 046215 (2010).
[14] S. Datta, G. W. Delius, R. Law, and M. J. Plank, J. Math. Bio. **63**, 779 (2011).
[15] L. Ridolfi, P. D'Odorico, and F. Laio, *Noise-Induced Phenomena in the Environmental Sciences* (Cambridge University Press, Cambridge, 2011).
[16] J. A. Bonachela, M. A. Muñoz, and S. A. Levin, J. Stat. Phys. **148**, 724 (2012).
[17] T. C. Butler, M. Benayoun, E. Wallace, W. van Drongelen, N. Goldenfeld, and J. Cowan, Proc. Natl. Acad. Sci. USA **109**, 606 (2012).
[18] A. J. McKane, T. Biancalani, and T. Rogers, Bull. Math. Biol. **76**, 895 (2014).
[19] D. T. Gillespie, A. Hellander, and L. R. Petzold, J. Chem. Phys. **138**, 170901 (2013).
[20] A. J. McKane and T. J. Newman, Phys. Rev. Lett. **94**, 218102 (2005).
[21] L. Ridolfi, C. Camporeale, P. D'Odorico, and F. Laio, Eur. Phys. Lett. **95**, 18003 (2011).
[22] L. Trefethen, A. Trefethen, S. Reddy, T. Driscoll, *et al.*, Science **261**, 578 (1993).
[23] L. N. Trefethen and M. Embree, *Spectra and pseudospectra: the behavior of nonnormal matrices and operators* (Princeton University Press, 2005).
[24] A. Roberts, The Journal of the Australian Mathematical Society. Series B. Applied Mathematics **31**, 48 (1989).
[25] M. G. Neubert and H. Caswell, Ecology **78**, 653 (1997).
[26] S. Tang and S. Allesina, Population Dynamics **2**, 21 (2014).
[27] M. G. Neubert, H. Caswell, and J. Murray, Mathematical biosciences **175**, 1 (2002).
[28] A. J. Roberts, *Model emergent dynamics in complex systems* (SIAM, Adelaide, 2014).
[29] B. F. Farrell and P. J. Ioannou, Phys. Rev. Lett. **72**, 1188 (1994).
[30] See Supplemental Material [url], which includes Refs. [32–34].
[31] The region of stochastic patterns is defined as the parameter regime in which the largest eigenvalue of $\boldsymbol{K}$ has a peak at some $\vec{k}_0 \neq 0$ with a value larger than its value at $\vec{k} = 0$.
[32] C. W. Gardiner, *Handbook of Stochastic Methods for Physics, Chemistry and the Natural Sciences*, 4th ed. (Springer, New York, 2009).
[33] N. G. van Kampen, *Stochastic Processes in Physics and Chemistry*, 3rd ed. (Elsevier Science, Amsterdam, 2007).
[34] M. Adam and M. J. Tsatsomeros, Electron. J. Linear Algebra **15**, 239 (2006).